PHYSICAL REVIEW D **83,** 111301(R) (2011)

Distinguishing nonuniversal models with polarized positron and electron beams

A. A. Bagneid* and N. A. Althubiti

Department of Physics, Umm Al-Qura University, Makkah, Saudi Arabia

(Received 4 March 2011; published 8 June 2011)

Gauge symmetries with nonuniversal couplings can manifest themselves in e^+e^- collisions via generation-dependent deviations of leptonic observables from the standard model predictions. We analyze the deviations in terms of the lepton couplings to the extra neutral gauge boson and the polarizations of the positron and electron beams. We show how the proper manipulation of both the nonuniversal couplings and the applied beam polarization can result in considerable improvement in the differentiation of the corresponding models and in the identification reach of the extra nonuniversal gauge boson.

DOI: 10.1103/PhysRevD.83.111301 PACS numbers: 12.15.Ji, 12.60.Cn, 13.88.+e, 14.70.Pw

In spite of the impressive experimental confirmations of the standard model (SM), there seems to be a general consensus that it is not the ultimate theory of fundamental interactions. Accordingly, new mechanisms of electroweak symmetry breaking are introduced. Most of these theories predict the existence of additional neutral gauge bosons, Z'. It is believed that if an additional neutral gauge boson exists, it should be observed through the Drell-Yan process at the present high-energy hadronic colliders, if its mass is in the few TeV range. The present Z' discovery limits at the Tevatron are $\sim$0.8–1 TeV [1]. On the other hand, as the integrated luminosity at the LHC [2] reaches $\sim$30–100 fb^{-1}, the discovery limits are expected to approach the few TeV range. For masses above these limits, a Z' search at the LHC may be provided by indirect means through deviations of cross sections from the SM predictions. However, the identification may be difficult because of limited statistics. Nevertheless, future e^+e^- linear colliders (LC) are considered necessary and proper to accomplish indirect searches for new Z'. LC are expected to make high precision measurements of any additional gauge bosons for their couplings and interactions with other particles. The need for high-energy LC is being addressed by the proposed International Linear Collider (ILC) [3], which is expected to operate with collision energies in the range 0.5–1 TeV. The energy frontier next to ILC is expected to be provided by the Compact Linear Collider (CLIC) [4], which is designed to operate at collision energies in the range 1–5 TeV. The possibility of beam polarization for both positrons and electrons in LC gives another advantage to enhance the discovery limits of Z'.

We are interested here in studying characteristic signals in e^+e^- collisions resulting from the presence of neutral gauge bosons that occur in models beyond the SM. In particular, we will consider family nonuniversal neutral gauge bosons and, as a case study, we will regard gauge bosons occurring in the minimal supersymmetric standard model (MSSM) [5] and in the $Sp(6)_L \otimes U(1)_Y$ model (SPM) [6].

*bagneid@yahoo.com

The general expression for the differential cross section for the process $e^+e^- \to \bar{\ell}\ell$, $\ell = \mu, \tau$ ($\ell \neq e$), when longitudinally polarized beams are employed and the helicities of the final states measured, is given by [7]

$$\frac{d\sigma^{\rm pol}}{d\Omega} = \frac{\alpha^2}{4s}[A(1+\cos^2\vartheta) + 2B\cos\vartheta]. \tag{1}$$

The functions A and B are given by

$$A = \lambda_1(h_1F_1 + h_2F_4) + \lambda_2(h_1F_3 + h_2F_2), \tag{2}$$

$$B = \lambda_1(h_1F_2 + h_2F_3) + \lambda_2(h_1F_4 + h_2F_1), \tag{3}$$

where $\lambda_1 = 1 - \lambda_+\lambda_-$, $\lambda_2 = \lambda_+ - \lambda_-$, $h_1 = (1 - h_+h_-)/4$, and $h_2 = (h_+ - h_-)/4$. Here λ_+ and λ_- denote the helicities of the incident positron and electron, while h_+ and h_- denote the helicities of the final $\bar{\ell}$ and ℓ leptons, respectively. Measurements of the helicities of the final state leptons, in particular, the tau leptons, are useful in distinguishing family nonuniversal models [8]. However we will be concerned here only with the helicities of the initial state leptons. Let Z_1 and Z_2, with masses M_1 and M_2, denote the mass eigenstate neutral gauge boson of the SM and of the additional neutral boson of the model under consideration, respectively. They represent mixtures of the weak eigenstate bosons with a mixing angle φ. Z_1 and Z_2 couple to fermion f through vector and axial-vector couplings (v_1^f, a_1^f) and (v_2^f, a_2^f), respectively. The functions F_n, $n = 1, 2, 3, 4$, are given by

$$F_1 = 1 + 2\sum_{j=1}^{2} v_j^e v_j^\ell \chi_j + \sum_{j,k=1}^{2} (\chi_j\chi_k + \eta_j\eta_k) \times (v_j^e v_k^e + a_j^e a_k^e)(v_j^\ell v_k^\ell + a_j^\ell a_k^\ell), \tag{4}$$

$$F_2 = 2\sum_{j=1}^{2} a_j^e a_j^\ell \chi_j + \sum_{j,k=1}^{2} (\chi_j\chi_k + \eta_j\eta_k)(v_j^e a_k^e + a_j^e v_k^e) \times (v_j^\ell a_k^\ell + a_j^\ell v_k^\ell), \tag{5}$$

$$F_3 = 2\sum_{j=1}^{2} a_j^e v_j^\ell \chi_j + 2\sum_{j,k=1}^{2} (\chi_j\chi_k + \eta_j\eta_k) \times v_j^e a_k^e (v_j^\ell v_k^\ell + a_j^\ell a_k^\ell), \tag{6}$$

$$F_4 = F_3(e \leftrightarrow \ell), \tag{7}$$

where the functions χ_i and η_i, $i = 1, 2$, are given in [9].

In what follows we will examine three classes of observables as predicted by the models under consideration. The first class, class (1), consists of the unpolarized cross section $\sigma(\ell) \equiv \sigma(e^+e^- \to \bar{\ell}\ell)$, forward-backward asymmetry $A_{\rm FB}(\ell) \equiv A_{\rm FB}(e^+e^- \to \bar{\ell}\ell)$, and the left-right asymmetry with a partially polarized electron beam and an unpolarized positron beam: $A^P_{\rm LR}(\ell) \equiv A^P_{\rm LR}(e^+e^- \to \bar{\ell}\ell)$, where P is the longitudinal degree of polarization. Class (2) observables, denoted by $\sigma^{\rm pol}(\ell)$, $A^{\rm pol}_{\rm FB}(\ell)$, and $A^{\rm pol}_{\rm LR}(\ell)$, consist of the same observables as class (1) but with the electron beam predominantly left-handed and the positron beam predominantly right-handed. Class (3) observables, denoted by $\sigma^{\rm rpol}(\ell)$, $A^{\rm rpol}_{\rm FB}(\ell)$, and $A^{\rm rpol}_{\rm LR}(\ell)$, consist of the same observables as class (2) but with the signs of polarization of the positron and electron beams reversed.

Let us parametrize the functions F_n, $n = 1, 2, 3, 4$, as follows:

$$F_n = \delta_{1,n} + \sum_{i=1}^{2} K^n_i(\ell) + \sum_{\substack{i,j=1 \\ j\geq i}}^{2} K^n_{ij}(\ell), \tag{8}$$

where the terms $K_i(\ell)$ and $K_{ij}(\ell)$ are given by

$$K^n_i(\ell) = C^n_i(\ell)\chi_i; \quad K^n_{ij}(\ell) = C^n_{ij}(\ell)(\chi_i\chi_j + \eta_i\eta_j) \quad j \geq i. \tag{9}$$

The dominant contribution to the cross sections on and within a few total widths of the Z_2 resonance peak is proportional to the parameter $r = R_1(\ell)R_2$, where $R_1(\ell) = C^1_{22}(\ell)/(\Gamma_2)^2$ and $R_2 = \lambda_1 + (A_{\rm LR}(\ell))_p\lambda_2$. Here, Γ_2 is the total width [10] of the Z_2 boson and $(A_{\rm LR}(\ell))_p$ is the left-right asymmetry on the resonance peak. $(A_{\rm LR}(\ell))_p = A_e$, where for fermion f, $A_f = 2[(x^f_2) + (x^f_2)^{-1}]^{-1}$ with $x^f_i = v^f_i/a^f_i$, $i = 1, 2$, and the subscript p refers to the peak value on top of the Z_2 resonance.

Let us now turn to our results. We start by investigating the on-resonance leptonic cross sections. In Figs. 1(a)–1(c) we present, respectively, the cross sections, $\sigma(\ell)$, $\sigma^{\rm pol}(\ell)$, and $\sigma^{\rm rpol}(\ell)$, $\ell = \mu, \tau$, for the models considered here, as functions of $\sqrt{s}$. For the on-resonance calculations, we will assume that $M \equiv M_2 = 1.5$ TeV and $\varphi = 0$. For class (2) observables we will take $\lambda_+ = +60\%$ and $\lambda_- = -80\%$. Figure 1(a) shows that, at resonance, $[\sigma_{\rm SPM}(\tau)]_p/[\sigma_{\rm SPM}(\mu)]_p \approx 4$ and $[\sigma_{\rm MSSM}(\mu)]_p/[\sigma_{\rm MSSM}(\tau)]_p \approx 6.5$. These results are in agreement with the predicted values: $(R_1(\tau)/R_1(\mu))_{\rm SPM} = 4$ and $(R_1(\mu)/R_1(\tau))_{\rm MSSM} = 6.5$. Figures 1(b) and 1(c) show that the ratio $[\sigma(\tau)]_p/[\sigma(\mu)]_p$ is unaffected by beam polarization. This result is expected because the factor R_2 is independent of the couplings of the final state lepton ℓ. Comparison of Figs. 1(a) and 1(b) gives the ratios $f^{\rm pol}_{\rm SPM}(\ell) \equiv [\sigma^{\rm pol}_{\rm SPM}(\ell)/\sigma_{\rm SPM}(\ell)]_p \approx 2.88$ and $f^{\rm pol}_{\rm MSSM}(\ell) \equiv [\sigma^{\rm pol}_{\rm MSSM}(\ell)/\sigma_{\rm MSSM}(\ell)]_p \approx 0.08$, $\ell = \mu, \tau$. These quite different behaviors are consistent with the predicted values: $f^{\rm pol}_{\rm SPM}(\ell) = (R_2)_{\rm SPM} = \lambda_1 + \lambda_2$ and $f^{\rm pol}_{\rm MSSM}(\ell) = (R_2)_{\rm MSSM} = \lambda_1 - \lambda_2$. As the signs of the polarization of the positron and electron beams are reversed [Fig. 1(c)], the sign of λ_2 is reversed. As a result we get $f^{\rm rpol}_{\rm SPM}(\ell) = \lambda_1 + \lambda_2 = 0.08$ and $f^{\rm rpol}_{\rm MSSM}(\ell) = \lambda_1 - \lambda_2 = 2.88$, $\ell = \mu, \tau$. These predictions are in agreement with Fig. 1(c).

The usual way for obtaining discovery limits for extra gauge bosons in e^+e^- collisions relies on distinguishing off-resonance values of observables as predicted by a given model, from the corresponding SM predictions. We instead suggest obtaining discovery limits by distinguishing predicted values of observables having a final dileptonic state that belongs to one generation from the corresponding values of the same observables but with a final dileptonic state that belongs to a different generation. By doing that, the discovery limits can significantly be improved depending on the splittings between the compared observables. The magnitudes of such splittings depend, in turn, on the signs and magnitudes of the deviations of the compared observables from the SM predictions which are determined through the functions $F'_n(\ell) = K^n_2(\ell) + K^n_{12}(\ell) + K^n_{22}(\ell)$, $n = 1, 2, 3, 4$. At the limit $M \gg \sqrt{s} \gg M_1$, with $\varepsilon = (a^e_1)^2/x(1-x)$ and $x = \sin^2\vartheta_W$, the sign of the deviation of $\sigma(\ell)$ from the SM predictions is that of the function

$$S(\ell) = -a^e_2 a^\ell_2\{x^e_2 x^\ell_2 + \varepsilon[1 + x^e_1 x^e_2][1 + x^e_1 x^\ell_2]\}, \tag{10}$$

except for the special cases in which $(x^e_2 = 0, x^\ell_2 = -(x^e_1)^{-1})$ or $(x^\ell_2 = 0, x^e_2 = -(x^e_1)^{-1})$, for which the deviations are expected to be positive and very small.

Let us begin our off-resonance investigations by examining class (1) and class (2) observables in the energy range $M \gg \sqrt{s} \gg M_1$. In Figs. 2 and 3 class (1) and class (2) observables are presented, respectively, for the considered models as functions of the gauge boson mass M, which is taken as a free parameter, where we take $\sqrt{s} = 0.5$ TeV.

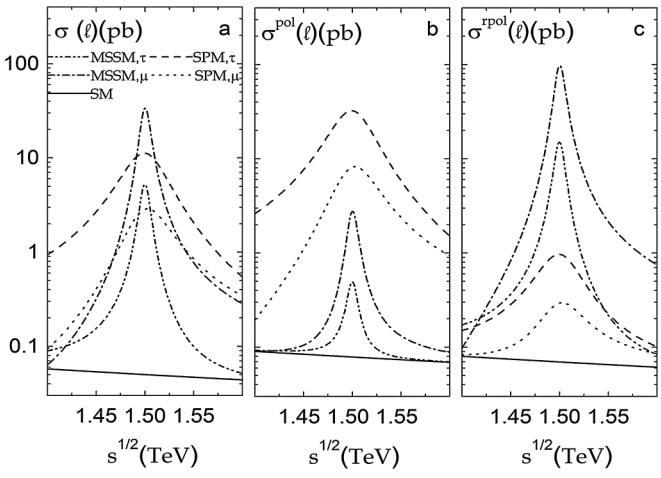

FIG. 1. The cross sections $\sigma(\ell)$ [panel (a)], $\sigma^{\rm pol}(\ell)$ [panel (b)], and $\sigma^{\rm rpol}(\ell)$ [panel (c)], $\ell = \mu, \tau$, as functions of $\sqrt{s}$, for the MSSM, the SPM, and the SM. We take $M = 1.5$ TeV and $\varphi = 0$.

Figure 2(a) shows large positive deviations for $[\sigma(\tau)]_{\rm SPM}$ from $[\sigma(\tau)]_{\rm SM}$. These large deviations are almost tripled after polarized beams are employed [Fig. 3(a)]: $f'^{\rm pol}_{\rm SPM}(\tau) \equiv \frac{\sigma^{\rm pol}_{\rm SPM}(\tau)-\sigma^{\rm pol}_{\rm SM}(\tau)}{\sigma_{\rm SPM}(\tau)-\sigma_{\rm SM}(\tau)} \approx 2.88$. On the other hand, there are relatively smaller corresponding positive deviations for $[\sigma(\tau)]_{\rm MSSM}$ that diminish when polarized beams are employed: $f'^{\rm pol}_{\rm MSSM}(\tau) \approx 0.08$. Similar results, but with negative deviations, are found for $f'^{\rm pol}_{\rm SPM}(\mu)$ and $f'^{\rm pol}_{\rm MSSM}(\mu)$. Now, for both models, the couplings are such that $S(\tau) > 0$ and $S(\mu) < 0$. Therefore, for both models, the deviations of $\sigma(\tau)$ are positive and those of $\sigma(\mu)$ are negative, as Fig. 2(a) shows. Next, we wish to compare the magnitudes of the deviations from the SM predictions, of cross sections belonging to different classes. For the SPM we find that $F'_1(\tau) = F'_3(\tau) > 0$ and $F'_1(\mu) = F'_3(\mu) < 0$. Similarly, for the MSSM, the couplings are such that $F'_1(\tau) = -F'_3(\tau) > 0$ and $F'_1(\mu) = -F'_3(\mu) < 0$. When polarized beams are employed [class (2)], we thus find the ratios $f'^{\rm pol}_{\rm SPM}(\ell) = \lambda_1 + \lambda_2$ and $f'^{\rm pol}_{\rm MSSM}(\ell) = \lambda_1 - \lambda_2$, $\ell = \mu, \tau$. These predictions agree with the above stated observations on Figs. 2(a) and 3(a).

Next we consider the forward-backward asymmetries at the limit $M \gg \sqrt{s} \gg M_1$. For example, the couplings in the SPM are such that $F'_1(\tau) = F'_2(\tau) > 0$ and $F'_1(\mu) = F'_2(\mu) < 0$. With $1 > [A_{\rm FB}(\ell)]_{\rm SM} > 0$ at the stated limit, it thus turns out that $[A_{\rm FB}(\tau)]_{\rm SPM} > [A_{\rm FB}(\tau)]_{\rm SM}$ and $[A_{\rm FB}(\mu)]_{\rm SPM} < [A_{\rm FB}(\mu)]_{\rm SM}$, as Fig. 2(b) shows. Trends similar to those encountered in the deviations of the cross sections from the SM predictions can be noticed for the forward-backward asymmetries, where Figs. 2(b) and 3(b) show that, by polarizing the beams [class (2)], the forward-backward asymmetries become further departed from the SM predictions for the SPM, and get closer to the SM predictions for the MSSM. However, the explanation of the deviation results in terms of the lepton couplings, and the beam polarization is not as transparent as in the case of the cross sections.

With the above given relations among $F'_1(\ell)$ and $F'_3(\ell)$, $\ell = \mu, \tau$, and with $1 > [A_{\rm LR}(\ell)]_{\rm SM} > 0$ at the stated limit, the deviations of the SPM left-right asymmetries from the SM predictions are positive for $\ell = \tau$ and negative for $\ell = \mu$. Similarly, for the MSSM, they are positive for $\ell = \mu$ and negative for $\ell = \tau$. When compared with $A^P_{\rm LR}(\ell)$, we find that $|A^{\rm pol}_{\rm LR}(\ell)| > |A^P_{\rm LR}(\ell)|$, as Figs. 2(c) and 3(c) show. This is expected since, with the given beam polarization, $A^{\rm pol}_{\rm LR}(\ell)/A^P_{\rm LR}(\ell) = P_{\rm eff}/P > 0$, where the effective polarization $P_{\rm eff} = \lambda_2/\lambda_1$.

The above results show that the MSSM observables give a low profile after the employment of polarized beams [class (2) observables]. In order to improve the results for the MSSM, we suggest employing class (3) observables. We display our results for class (3) observables in Fig. 4. Because of coupling considerations, the SPM observables show lower predictions. Figures 2(a) and 4(a) show that

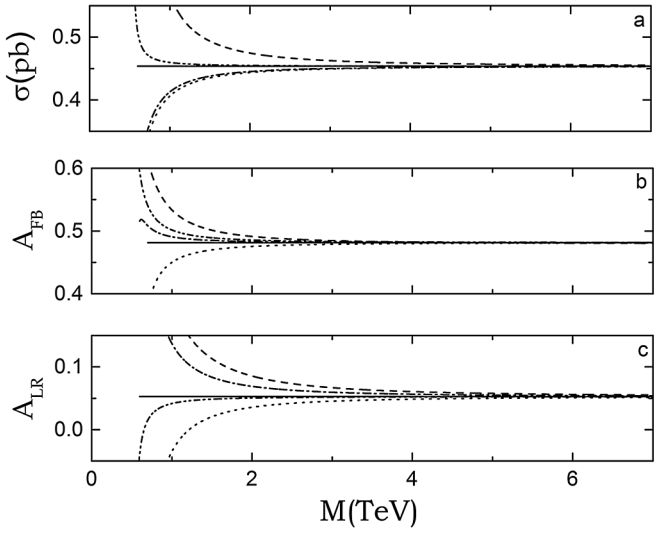

FIG. 2. The observables $\sigma(\ell)$, $A_{\rm FB}(\ell)$, and $A^P_{\rm LR}(\ell)$, with $\ell = \mu$, τ, and $P = 80\%$ as predicted by the models considered in the text, as functions of M for $\sqrt{s} = 500$ GeV. The curve notations are the same as in Fig. 1.

$f'^{\rm rpol}_{\rm MSSM}(\ell) \approx 2.88$ and $f'^{\rm rpol}_{\rm SPM}(\ell) \approx 0.08$, $\ell = \mu, \tau$. With λ_2 now negative, the above observations are consistent with the predicted values: $f'^{\rm rpol}_{\rm MSSM}(\ell) = \lambda_1 - \lambda_2$ and $f'^{\rm rpol}_{\rm SPM}(\ell) = \lambda_1 + \lambda_2$. An improvement can also be noticed in Fig. 4(b) for $[A^{\rm rpol}_{\rm FB}(\ell)]_{\rm MSSM}$, as compared with the corresponding class (1) observable. We note that the predictions for $A^{\rm rpol}_{\rm LR}(\ell)$ [Fig. 4(c)] are related to $A^{\rm pol}_{\rm LR}(\ell)$ by just a negative sign.

In what follows, we will obtain two classes of identification reaches for the gauge bosons $Z_2 = Z_{\rm MSSM}$ and $Z_2 = Z_{\rm SPM}$. We obtain discovery limits M_d by constructing the χ^2 figure of merit that determines the Z_2 masses up to

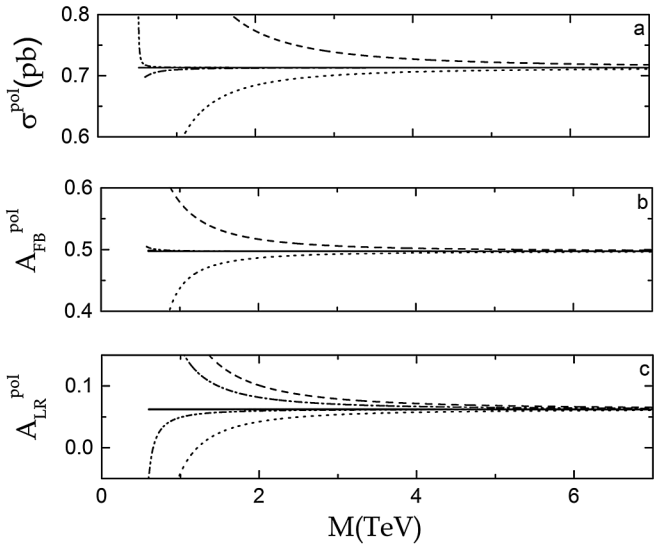

FIG. 3. Same as Fig. 2 but for the observables $\sigma^{\rm pol}(\ell)$, $A^{\rm pol}_{\rm FB}(\ell)$, and $A^{\rm pol}_{\rm LR}(\ell)$, with $\lambda_+ = +60\%$ and $\lambda_- = -80\%$, The curve notations are the same as in Fig. 1.

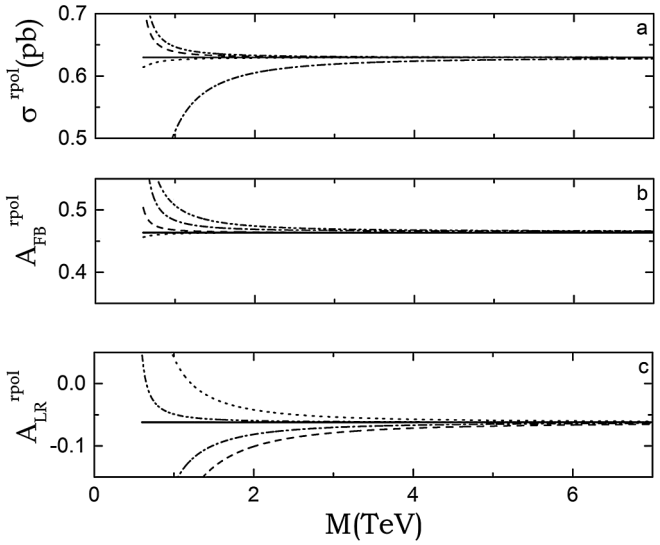

FIG. 4. Same as Fig. 2 but for the observables $\sigma^{\rm rpol}(\ell)$, $A_{\rm FB}^{\rm rpol}(\ell)$, and $A_{\rm LR}^{\rm rpol}(\ell)$, with $\lambda_+ = -60\%$ and $\lambda_- = +80\%$. The curve notations are the same as in Fig. 1.

which the observables considered here can statistically be distinguished from the corresponding predictions of the SM. We also obtain $\mu - \tau$ distinguishability limits, $M_{\mu-\tau}$, by constructing the $\chi^2_{\mu-\tau}$ figure of merit that determines the Z_2 masses up to which the observables that have τ pairs in their final states (the τ observables) can statistically be distinguished from the corresponding μ observables [9,11]. It is interesting to examine the contributions to χ^2 due to different observables. As for $Z_{\rm SPM}$, Fig. 5 shows significant improvement for χ^2 due to the employment of polarized beams [class (2)]. Moreover, the largest contributions to χ^2 come from the τ observables, as expected. For $Z_{\rm MSSM}$, Fig. 6 shows that the dominant contributions to χ^2 come from $\sigma(\mu)$ and $A_{\rm LR}(\mu)$ for the class (1) observables and from $\sigma^{\rm rpol}(\mu)$ and $A_{\rm LR}^{\rm rpol}(\mu)$ for the class (3) observables, in agreement with Figs. 2 and 4.

We calculated the 99% C.L. discovery limits M_d and $M_{\mu-\tau}$ for $Z_{\rm SPM}$ and $Z_{\rm MSSM}$, in future planned and proposed e^+e^- colliders. The results are displayed in Figs. 7 and 8, respectively. These figures show that, for both models, the employment of polarized beams [class (2) for $Z_{\rm SPM}$ and class (3) for $Z_{\rm MSSM}$] improved the discovery limits M_d by almost ~50%. Moreover, the discovery limits obtained on the basis of distinguishing the τ versus μ observables, $M_{\mu-\tau}$, added ~15% improvement for $Z_{\rm SPM}$ with class (2) observables and ~5% for $Z_{\rm MSSM}$ with class (3) observables. For example, at $\sqrt{s} = 0.5$ TeV with luminosity $L = 0.5$ ab^{-1}, the discovery limits for $Z_{\rm SPM}$ jumped from $M_d \approx 6.5$ TeV for class (1) observables up to $M_{\mu-\tau} \approx 11$ TeV for class (2) observables. At $\sqrt{s} = 3$ TeV and $L = 1$ ab^{-1} Fig. 7 shows that the CLIC is expected to be able to probe $Z_{\rm SPM}$ masses up to $M_{\mu-\tau} \approx 32.3$ TeV with class (2) observables. As for the MSSM, Fig. 8 shows that the corresponding results, but with class (3) observables replacing class (2) observables, are $M_d \approx 4.1$ TeV, $M_{\mu-\tau} \approx 6.4$ TeV, and $M_{\mu-\tau} \approx 18.8$ TeV. In the above calculations we considered only statistical errors. It has been shown that the inclusion of the systematic errors reduces the limits substantially [9]. Systematic errors will therefore have to be kept under control.

In conclusion, we studied measurable observables in e^+e^- collisions, having final state dileptons produced by family nonuniversal neutral gauge bosons Z_2 and the SM gauge boson Z_1. The observables were categorized into

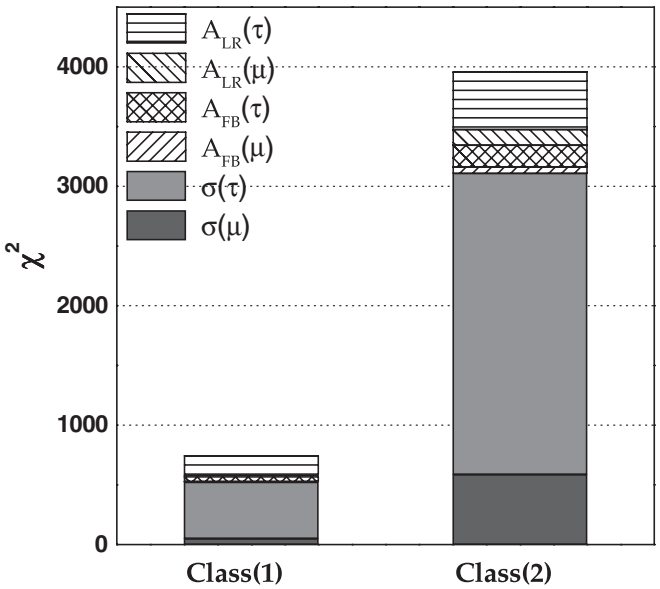

FIG. 5. The contributions to χ^2 from class (1) and class (2) observables, for the SPM. These are based on $\sqrt{s} = 0.5$ TeV and $M = 2$ TeV.

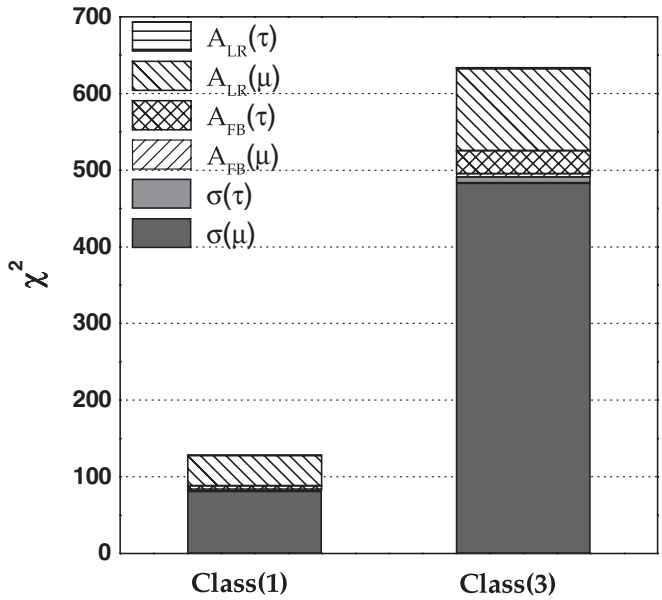

FIG. 6. The contributions to χ^2 from class (1) and class (3) observables, for the MSSM. These are based on $\sqrt{s} = 0.5$ TeV and $M = 2$ TeV.

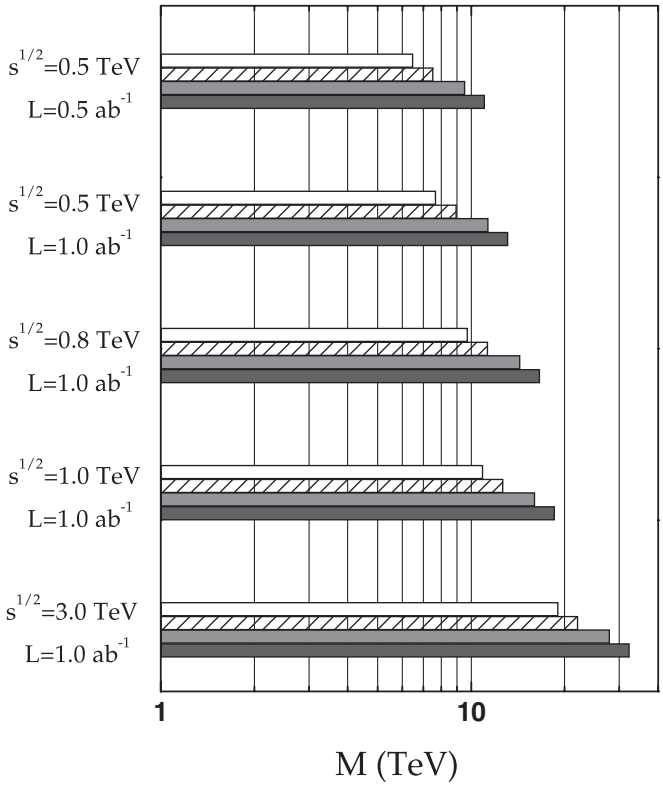

FIG. 7. Discovery limits for Z_{SPM} at high-energy e^+e^- colliders. The limits are 99% C.L. obtained from a χ^2 based on class (1) observables (open bars), distinguishing the μ and τ observables of class (1) (hatched bars), class (2) observables (shaded bars) and distinguishing the μ and τ observables of class (2) (solid bars).

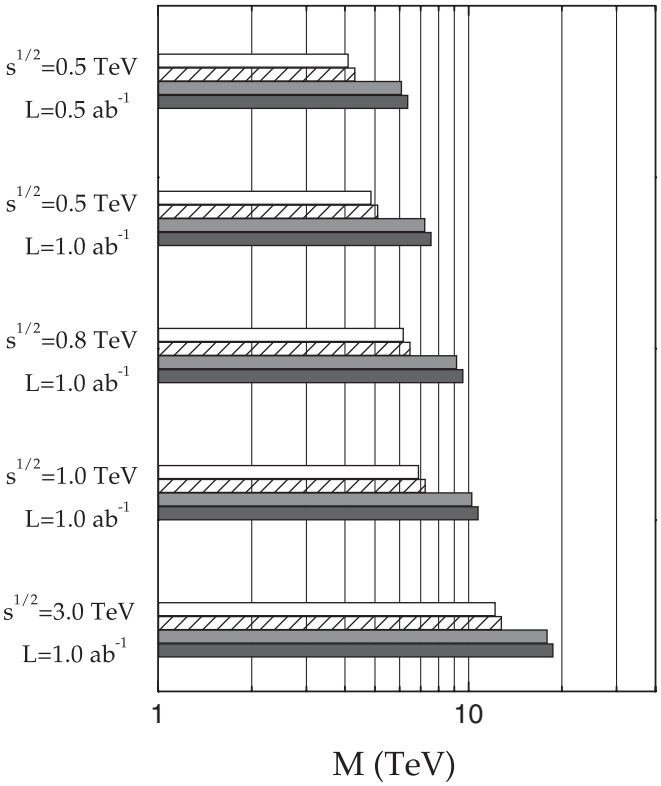

FIG. 8. Same as Fig. 7 but for Z_{MSSM} with class (3) observables replacing class (2) observables.

classes according to the polarizations of the positron and electron beams. Because of the generation-dependent couplings of leptons to Z_2, relative enhancements are expected in the on-Z_2 resonance unpolarized cross sections for production of lepton pairs belonging to different generations. The polarization of the beams causes a shift in the on-resonance leptonic cross sections. The sign and magnitude of this shift do not depend on the final dileptonic state, but rather on the specific polarizations of the positron and electron beams and on the electronic couplings to the extra gauge boson. We studied the observables off and away from the Z_1 and Z_2 resonances. The signs and relative magnitudes of the deviations from the SM predictions, of observables belonging to different classes, are determined by examining the contributions in the expressions of these observables due to the presence of Z_2. We found that by the proper utilization of the nonuniversal couplings and the appropriate adjustment of the beam polarization, both the identification and the discovery limits of Z_2 can gain considerable improvement.

[1] See, for example, T. Aaltonen *et al.*, Phys. Rev. Lett. **99**, 171802 (2007).
[2] See, for example, http://lhc.web.cern.ch/lhc/.
[3] See, for example, http://www.linearcollider.org/cms/.
[4] See, for example, http://clic-study.org/; A. Accomando *et al.*, CLIC Physics Group, arXiv:hep-ph/0412251.
[5] D. A. Demir, G. L. Kane, and T. T. Wang, Phys. Rev. D **72**, 015012 (2005); A. Hayreter, Phys. Lett. B **649**, 191 (2007).
[6] See, for example, T. K. Kuo and N. Nakagawa, Phys. Rev. D **31**, 1161 (1985); Nucl. Phys. **B250**, 641 (1985); A. Bagneid *et al.*, Int. J. Mod. Phys. A **2**, 1351 (1987).
[7] See, for example, W. Hollik, Z. Phys. C **8**, 149 (1981); A. Leike, Phys. Rep. **317**, 143 (1999); G. T. Park and T. K. Kuo, Phys. Rev. D **45**, 1720 (1992).
[8] See, for example, G. T. Park and T. K. Kuo, Phys. Rev. D **45**, 1720 (1992).
[9] A. A. Bagneid, Eur. Phys. J. C **54**, 547 (2008).
[10] For width calculations, see, for example, A. Leike, Phys. Rep. **317**, 143 (1999).
[11] A. A. Bagneid and N. A. Althubiti, AIP Conf. Proc. (to be published).